JACS
JOURNAL OF THE AMERICAN CHEMICAL SOCIETY
Article
pubs.acs.org/JACS

Selective Hydrogen Production from Formic Acid Decomposition on Pd−Au Bimetallic Surfaces

Wen-Yueh Yu,[†] Gregory M. Mullen,[†] David W. Flaherty,[‡] and C. Buddie Mullins*[,†]

[†]McKetta Department of Chemical Engineering and Department of Chemistry, Center for Nano and Molecular Science and Technology, Texas Materials Institute, and Center for Electrochemistry, University of Texas at Austin, Austin, Texas 78712, United States

[‡]Department of Chemical & Biomolecular Engineering, University of Illinois at Urbana—Champaign, Urbana, Illinois 61801, United States

Supporting Information

ABSTRACT: Pd−Au catalysts have shown exceptional performance for selective hydrogen production via HCOOH decomposition, a promising alternative to solve issues associated with hydrogen storage and distribution. In this study, we utilized temperature-programmed desorption (TPD) and reactive molecular beam scattering (RMBS) in an attempt to unravel the factors governing the catalytic properties of Pd−Au bimetallic surfaces for HCOOH decomposition. Our results show that Pd atoms at the Pd−Au surface are responsible for activating HCOOH molecules; however, the selectivity of the reaction is dictated by the identity of the surface metal atoms adjacent to the Pd atoms. Pd atoms that reside at Pd−Au interface sites tend to favor dehydrogenation of HCOOH, whereas Pd atoms in Pd(111)-like sites, which lack neighboring Au atoms, favor dehydration of HCOOH. These observations suggest that the reactivity and selectivity of HCOOH decomposition on Pd−Au catalysts can be tailored by controlling the arrangement of surface Pd and Au atoms. The findings in this study may prove informative for rational design of Pd−Au catalysts for associated reactions including selective HCOOH decomposition for hydrogen production and electro-oxidation of HCOOH in the direct formic acid fuel cell.

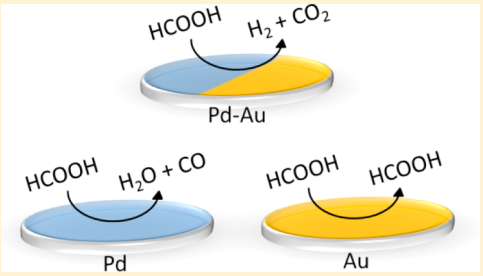

1. INTRODUCTION

Hydrogen is a promising energy carrier for electricity generation in a fuel cell; however, hydrogen storage and distribution remains a challenging issue. Recently, formic acid (HCOOH) has been proposed as a potential liquid storage medium capable of releasing H_2 under mild conditions via catalytic decomposition.[1−5] For practical applications, suitable catalysts are essential to facilitate HCOOH decomposition via dehydrogenation (HCOOH → H_2 + CO_2) as opposed to dehydration (HCOOH → H_2O + CO). Recently, considerable advances have been made in the selective dehydrogenation of HCOOH at ambient and near-ambient temperatures using homogeneous catalysts.[6−9] Nevertheless, the separation issues associated with homogeneous catalysts and requisite use of organic solvents and additives hamper their practical applications.[10,11] Use of heterogeneous catalysts may circumvent these issues, but improved catalytic performance under ambient conditions is still required.[10,11]

Pd is one of the most active catalysts for HCOOH decomposition.[11] Recently, heterogeneous catalysts containing Pd have been extensively studied for H_2 production via HCOOH decomposition;[11−23] among them, Pd−Au bimetallic catalysts have received substantial attention due to their promising performance in selective HCOOH dehydrogenation.[12−15,22,23] Yet, the key factors controlling the catalytic performance (e.g., activity and selectivity) of Pd−Au bimetallic catalysts on HCOOH decomposition remain topics of debate.[11−13,15,19,22,23] For instance, Pd−Au alloy catalysts were reported to possess improved HCOOH dehydrogenation activity and stability relative to monometallic Pd catalysts.[12,15,22] Such improvement has been attributed to a higher resistance to CO poisoning due to alloying of Pd with Au.[12,15] However, a recent study indicated that alloying of Pd with Au leads to lower HCOOH decomposition activity, which was suggested to result from a ligand effect as indicated by a slight shift of the Pd $3d_{5/2}$ binding energy in X-ray photoelectron spectroscopy (XPS).[19] Apart from alloy catalysts, supported Pd−Au catalysts with core−shell structures were also tested for selective HCOOH decomposition;[11,13,23] a higher hydrogen yield was observed[13,23] and attributed to the possible charge transfer between Au and Pd (i.e., a ligand effect).[23] However, it has been shown that the charge transfer between Au and Pd is insignificant owing to similar work functions between the Au and the Pd,[11] and a lower rate of HCOOH decomposition was observed for the colloidal Au−Pd core−shell nanoparticles relative to colloidal Pd nanoparticles.[11] The inconsistencies between these studies may be due to the vast diversity of preparation methods, catalyst supports, and reaction conditions employed in these studies. Indeed, classical heterogeneous

Received: May 23, 2014
Published: July 14, 2014

   dx.doi.org/10.1021/ja505192v | J. Am. Chem. Soc. 2014, 136, 11070−11078

catalysts are generally complex and operate at high temperatures and pressures, increasing the level of difficulty to unravel the factors governing the catalytic properties (e.g., reactivity and selectivity). In model catalyst studies, reactions are investigated on well-defined single-crystal surfaces under ultrahigh vacuum (UHV) conditions, which enable thorough surface characterization, precise control of reactant coverages, and minimal environmental interference, thereby allowing the study between surface structures and catalytic properties of catalytic materials at the molecular level.[24−29]

In this study, the surface chemistry of HCOOH on Pd−Au bimetallic model surfaces was investigated using temperature-programmed desorption (TPD) and reactive molecular beam scattering (RMBS) methods in an attempt to improve the fundamental understanding of the selective decomposition of HCOOH on Pd−Au catalysts. A variety of Pd−Au bimetallic surfaces, prepared by varying the Pd coverage deposited on the Au(111) surface followed by annealing, were characterized by H_2-TPD and tested via HCOOH-RMBS and HCOOH-TPD under UHV conditions. Two types of surface sites, i.e., Pd−Au interface sites and Pd(111)-like sites (sites that lack neighboring Au atoms), were characterized qualitatively and quasi-quantitatively for the Pd−Au surface by H_2-TPD. Reactivity tests based on HCOOH-RMBS demonstrate the critical role of Pd−Au interface sites for selective hydrogen production via catalytic HCOOH dehydrogenation. Although increasing the fraction of Pd(111)-like sites on the surface increased the rate of HCOOH decomposition, the selectivity toward hydrogen production decreased because the Pd(111)-like sites primarily catalyze dehydration of HCOOH. HCOOH-TPD results reveal that reaction-limited desorption of CO_2 occurred at a relatively low temperature, indicating that the reaction intermediate(s) from HCOOH decomposition could be readily decomposed on the Pd−Au surface. These observations suggest that the exceptional performance of Pd−Au catalysts for selective HCOOH decomposition could be rationalized by the "ensemble" effect. The experimental results shown in this study provide direct evidence that the selectivity for HCOOH reaction pathways can be tailored by the intermixing of Pd and Au atoms on catalytically active surfaces, which is consistent with predictions from a recent theoretical study.[30]

2. EXPERIMENTAL METHODS

All experiments in this study were conducted in a molecular beam surface scattering apparatus with a base pressure of less than 1×10^{-10} Torr.[31−35] Briefly, the apparatus contains an Auger electron spectrometer (Physical Electronics 10−500), a quadrupole mass spectrometer (Extrel C-50), a Fourier transform infrared spectrometer (Bruker Tensor 27) combined with a mercury−cadmium−telluride (MCT) detector (Infrared Associates), as well as nozzles and apertures for generating two separate molecular beams.

The Au(111) single-crystal sample is a circular disk (Princeton Scientific, 12 mm in diameter × 2 mm thick) and held in place by a Mo wire fitted around a groove cut into the side of the sample. This wire is also used to resistively heat the sample and provide thermal contact between the sample and a liquid nitrogen bath for cooling. The temperature of the sample was measured with a K-type (Alumel−Chromel) thermocouple placed into a small hole in the edge of the disk-shaped sample. The Au(111) surface was periodically cleaned by Ar ion bombardment (2 keV), carried out at room temperature, followed by an anneal to 800 K. The cleanliness of the surface was verified by Auger electron spectroscopy (AES) with a beam energy of 3 keV and emission current of 1.5 mA.

Pd−Au model surfaces were prepared by depositing Pd atoms from a homemade thermal evaporator onto the Au(111) surface at 77 K and then annealing the surface to 500 K for 10 min under UHV conditions. The deposition rate of Pd was calibrated with a quartz crystal microbalance (QCM) controller (Maxtek Inc.) by assuming that the thickness of 1 monolayer (ML) of Pd is equal to the diameter of a Pd atom, which is 0.274 nm. Growth of the Pd overlayer on the Au(111) surface at 77 K is believed to obey a layer-by-layer mechanism based on a previous study[36] in which a Pd film was grown on the Au(111) surface at the higher temperature of 150 K. Upon annealing, some of the surface Pd atoms diffuse into the subsurface of the Au(111) sample, forming a Pd−Au alloy surface.[34−38] AES spectra for the as-deposited and annealed Pd/Au(111) surfaces are shown in the Supporting Information (Figure S1).

Temperature-programmed desorption (TPD) is a useful tool for providing information concerning the interactions between the surface (adsorbent) and the adsorbed species (adsorbate).[39−41] In the TPD measurement, a temperature ramp is applied to the surface and the rate of desorbing molecules is measured by monitoring the increase in evolving gas-phase species as a function of surface temperature using a mass spectrometer. Analyses of a series of TPD spectra can provide information such as the activation energy for desorption, the strength of the adsorbate−adsorbent interaction, and the relative surface coverage of adsorbate.[39−41] The interactions (i.e., adsorption, absorption, diffusion, and desorption) of hydrogen with Pd/Au(111) surfaces have been studied previously using H_2-TPD.[34] In this study, H_2-TPD was conducted to characterize the annealed Pd/Au(111) surfaces for qualitative and quasi-quantitative analyses of surface sites. Hydrogen was dosed by impinging a molecular beam of H_2 onto the Pd−Au surface at a surface temperature of 77 K to yield a saturation coverage. Afterward, the H-presaturated surface was heated to 500 K at a rate of 1 K/s, while the signal for $m/z^+ = 2$ (H_2) was monitored by a quadrupole mass spectrometer (QMS).

Application of molecular beam methods to well-defined model catalysts enables the detailed investigation of the chemical kinetics of surface reactions.[42,43] By correlating the chemical kinetics with the surface structure, mechanistic insights into the kinetic phenomena on catalyst surfaces can be obtained.[42,43] In this study, we used reactive molecular beam scattering (RMBS) to acquire kinetic information (i.e., HCOOH decomposition rate and turnover frequency for hydrogen production) on our Pd−Au surface. HCOOH-RMBS experiments were conducted by impinging a molecular beam of HCOOH onto the sample surface that was held at a temperature of 500 K. The flux of the HCOOH beam was estimated to be $\sim 5 \times 10^{14}$ molecules cm^{-2} s^{-1} using HCOOH-TPD spectra from the clean Au(111) surface (Figure S2, Supporting Information) and assuming 1 ML of HCOOH equals $\sim 1.39 \times 10^{15}$ molecules cm^{-2} (the surface atom density of Au(111)). Prior to exposure to the sample surface, the HCOOH beam was first impinged onto an inert stainless steel flag that was held in front of the sample to establish baseline signals. Products and unreacted HCOOH molecules were detected by monitoring the following QMS signals for each species: HCOOH ($m/z^+ = 46$, 44, 29, and 28), CO_2 ($m/z^+ = 44$ and 28), H_2 ($m/z^+ = 2$), CO ($m/z^+ = 28$), and H_2O ($m/z^+ = 18$). The amount of each species is proportional to the integral of its QMS intensity. The integrals of QMS intensities for CO_2 ($m/z^+ = 44$) and CO ($m/z^+ = 28$) were corrected by considering the contribution from the corresponding mass fragments of HCOOH and those from HCOOH and CO_2, respectively.

HCOOH-TPD was carried out by adsorbing HCOOH onto the sample surface at 77 K via a molecular beam followed by annealing to 500 K at a rate of 1 K/s. The QMS signals during HCOOH-TPD were detected in a manner similar to that described for HCOOH-RMBS experiments. The coverage of the HCOOH overlayer was determined by TPD of HCOOH from the clean (Pd-free) Au(111) surface (Figure S2, Supporting Information).

3. RESULTS AND DISCUSSION

3.1. H_2-TPD from Pd−Au Surfaces. In order to establish a structure−activity relationship for HCOOH decomposition on

dx.doi.org/10.1021/ja505192v | J. Am. Chem. Soc. 2014, 136, 11070−11078

the Pd−Au surface, a characterization technique that can provide both qualitative and quantitative information on surface properties is essential. Probe molecules such as CO and H_2 are commonly used to characterize the structure and composition of catalytic surfaces.

Adsorption of CO on the Pd−Au model surface has been extensively studied using CO-RAIRS (reflection−absorption infrared spectroscopy)[35,38,44−47] and CO-TPD.[35,44,47−49] Using CO-RAIRS, qualitative information such as the type of adsorption sites occupied by CO (e.g., atop sites, 2-fold or 3-fold bridge sites) on the Pd−Au surface can be inferred by the intramolecular CO stretch frequency[35,38,44−47] due to varying degrees of π-antibonding back-donation from the surface electrons; however, it has been shown that quantitative analysis using CO-RAIRS becomes difficult when contiguous Pd sites are present on the Pd−Au surface, probably due to the vibrational coupling effect that attenuates the IR intensity at high surface CO coverages.[45] Quantitative analysis based on CO-TPD is complicated for the annealed Pd/Au(111) surfaces as the CO desorption peak is fairly broad[35] (likely as a result of the superposition of multiple CO desorption peaks), making the surface site assignment and peak deconvolution difficult.

The interaction of hydrogen with the Pd−Au model surface has been investigated using H_2-TPD.[34,50−52] In a previous study using H_2-TPD we showed that the presence of contiguous Pd atoms (characterized by CO-RARIS) on the annealed Pd/Au(111) surfaces is crucial for dissociative adsorption of hydrogen molecules at 77 K.[34] Upon heating, hydrogen adatoms recombinatively desorb from the Pd−Au surface. According to the desorption temperature of hydrogen, two distinct surface sites, i.e., Pd−Au interface and Pd(111)-like sites (lacking adjacent Au atoms), were qualitatively assigned.[34] Furthermore, a quasi-quantitative analysis is feasible by performing peak deconvolution for the H_2-TPD spectra. Accordingly, here we utilized H_2-TPD to characterize the Pd−Au surfaces that were generated by annealing the as-deposited Pd/Au(111) surfaces in UHV.

Figure 1 depicts the H_2-TPD spectra for desorption of saturation coverages of hydrogen from the annealed Pd−Au surfaces with initial Pd coverages ranging from 0 to 4 ML. The annealed 1 ML Pd/Au(111) surface exhibited a broad H_2-TPD peak centered at ∼208 K. Since this hydrogen desorption temperature lies between those for Au(111) (∼108 K)[53] and Pd(111) surfaces (∼310−320 K),[50,54] we speculate that this desorption site consists of Au and Pd atoms and hydrogen desorption likely occurs at the interface between Au and Pd atoms.[34] This H_2-TPD feature is relatively broad because the desorption temperature of hydrogen depends on the relative number of Pd and Au atoms associated with the Pd−Au interface sites during the desorption process. In general, a higher hydrogen desorption temperature would be expected when H atoms bind to more Pd atoms in the Pd−Au interface sites since the bond strength of Pd−H is stronger than that of Au−H. For the annealed 2 ML Pd/Au(111) surface, the peak of hydrogen desorption from the Pd−Au interface sites (at ∼210 K) intensified and an additional shoulder at a higher temperature (∼300 K) was observed. The desorption temperature of this high-temperature shoulder is fairly close to the desorption temperature of hydrogen from the Pd(111) surface,[50,54] which suggests formation of Pd(111)-like sites on the annealed 2 ML Pd/Au(111) surface. Both hydrogen desorption features (i.e., from the Pd−Au interface and Pd(111)-like sites) grew in intensity on the Pd−Au surfaces prepared with higher initial Pd coverages of 3 and 4 ML.

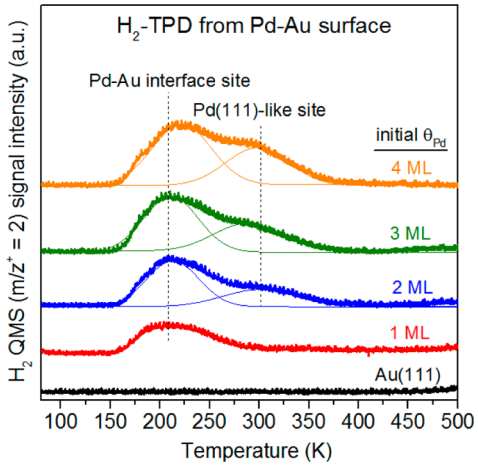

Figure 1. H_2-TPD spectra from Pd−Au surfaces with initial Pd coverages ranging from 0 to 4 ML. Pd−Au surfaces were prepared by depositing Pd atoms onto the Au(111) surface at a surface temperature (T_S) of 77 K followed by annealing to 500 K in UHV. A molecular beam of H_2 was impinged onto each surface at T_S = 77 K to yield a saturation coverage of H adatoms. Heating rate was 1 K/s.

The integral of the peak area under each H_2-TPD trace is proportional to the amount of hydrogen that desorbed from each Pd−Au surface.[39−41] It is noted that no measurable H_2 desorption was observed from the clean (Pd-free) Au(111) surface under the same set of conditions. In other words, the surface sites for hydrogen uptake are associated with surface Pd atoms. Sykes and co-workers[55,56] employed scanning-tunneling microscopy (STM) to observe H adatoms on Pd/Au(111) surfaces. STM imaging revealed that hydrogen molecules dissociatively adsorb on surface Pd atoms, and no spillover onto the Au terrace sites was observed.[55,56] Therefore, the integral peak area under each H_2-TPD trace should also reflect the relative number of surface Pd atoms for dissociative adsorption of hydrogen. By integrating the peak for H_2-TPD spectra, the relative number of surface Pd atoms on each Pd−Au surface was calculated (relative to that of the annealed 4 ML Pd/Au(111) surface). As listed in Table 1, the relative number of surface Pd atoms is 0.32, 0.63, 0.84, and 1 for the Pd−Au surface with the initial Pd coverage of 1, 2, 3, and 4 ML, respectively.

Dispersion, defined as the fraction of atoms of a material exposed to the surface, is an important indicator in heterogeneous catalysis since catalytic reactions occur on surfaces. For supported Pd catalysts, dispersion is generally expressed as the ratio of the amount of hydrogen uptake (determined from hydrogen chemisorption) to the total amount of Pd. In this study, the relative dispersion was computed by dividing the relative number of surface Pd atoms (determined from H_2-TPD) on each Pd−Au surface by its initial Pd coverage (relative to that of the annealed 4 ML Pd/Au(111) surface). The relative dispersion was found to gradually decrease as the initial Pd coverage was increased (Table 1), suggesting that a higher portion of Pd atoms was not surface accessible when the Pd−Au surface was prepared with a higher initial Pd coverage.

In order to quantify the relative number of Pd−Au interface and Pd(111)-like sites on each Pd−Au surface, the H_2-TPD spectra in Figure 1 were fitted by peak deconvolution, and the

dx.doi.org/10.1021/ja505192v | J. Am. Chem. Soc. 2014, 136, 11070−11078

Table 1. Relative Number of Surface Pd Atoms, Relative Dispersion, Fraction of Pd−Au Interface Sites, HCOOH Conversion, HCOOH Decomposition Rate, Turnover Frequency for H_2 Production, and Relative H_2/CO QMS Ratio on the Annealed Pd/Au(111) Surfaces

initial θ_{Pd} (ML)	relative no. of surface Pd atoms $(-)^{a,b}$	relative dispersion $(-)^{a,b}$	fraction of Pd−Au interface sites $(-)^{b}$	HCOOH conversion $(\%)^{c}$	HCOOH decomposition rate (HCOOH cm^{-2} $s^{-1})^{c}$	TOF for H_2 production (H_2 Pd_S^{-1} $s^{-1})^{b,c}$	Relative H_2/CO QMS ratio $(-)^{a,c}$
1	0.32	1.29	1	0.7	3.5×10^{12}	0.006	2.08
2	0.63	1.26	0.66	2.8	1.4×10^{13}	0.012	1.19
3	0.84	1.12	0.62	6.7	3.3×10^{13}	0.011	1.05
4	1	1	0.60	8.8	4.4×10^{13}	0.009	1

[a]Relative to that of the annealed 4 ML Pd/Au(111) surface. [b]Determined from H_2-TPD spectra (Figure 1). [c]Determined from HCOOH-RMBS spectra (Figure 3).

corresponding peak integrals are displayed in Figure 2. As the initial Pd coverage was increased, the amount of hydrogen

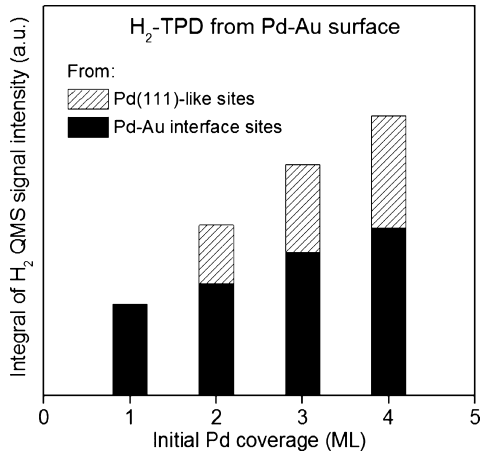

Figure 2. Integrals of H_2 QMS signal intensity for H_2-TPD spectra shown in Figure 1 after peak deconvolution.

desorption from the Pd−Au interface and Pd(111)-like sites both increased (Figure 2), indicating that the number of both types of surface sites increased since the amount of hydrogen desorption is proportional to the number of surface sites. The fraction of Pd−Au interface sites on each Pd−Au surface was calculated by the integral of hydrogen desorption from Pd−Au interface sites divided by that of the total hydrogen desorption from both Pd−Au interface and Pd(111)-like sites. The fraction of Pd−Au interface sites is unity for the annealed 1 ML Pd/Au(111) surface and reduces to ∼0.6 for surfaces with higher initial Pd coverages, i.e., 2−4 ML (see Table 1).

3.2. HCOOH-RMBS on Pd−Au Surfaces. The reactivity of HCOOH on Pd−Au surfaces was evaluated by HCOOH-RMBS. A room-temperature beam of HCOOH vapor was generated with a translational energy of ∼0.1 eV. The trapping probability of HCOOH under these conditions will be very close to unity regardless of the surface temperature. At elevated surface temperatures trapped molecules will undergo a kinetic competition between surface reaction and desorption.[57−60]

Figure 3 shows the HCOOH-RMBS results for annealed Pd/Au(111) surfaces with various initial Pd coverages. The HCOOH beam was first impinged onto the inert stainless steel flag that was held in front of the sample for 5 s (from 30 to 35 s) to establish baseline signals and then impinged onto the Pd−Au surface that was held at a surface temperature at 500 K for 5 s (from 65 to 70 s) to complete a King and Wells measurement.[61,62]

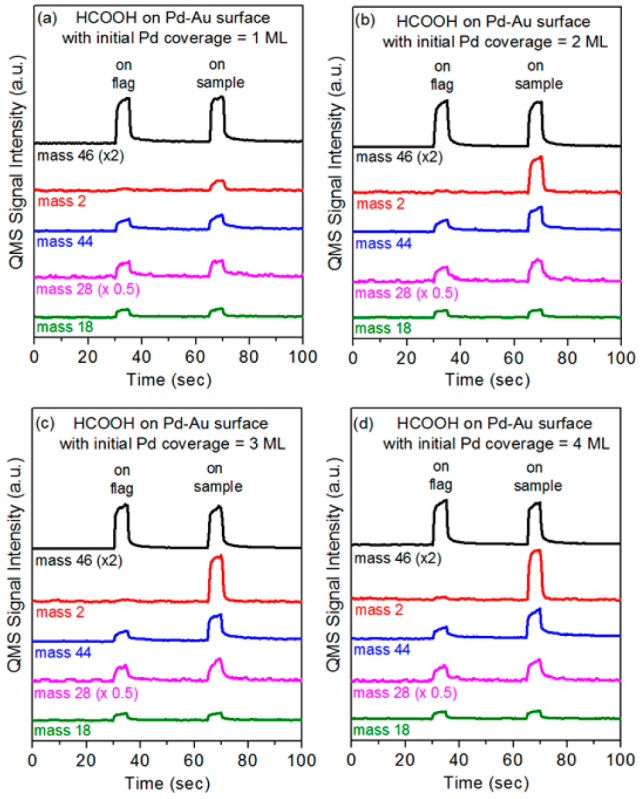

Figure 3. HCOOH-RMBS results for Pd−Au surfaces with various initial Pd coverages. Pd−Au surfaces were prepared by depositing Pd atoms onto the Au(111) surface at a surface temperature of 77 K followed by annealing to 500 K in UHV. The surface was held at 500 K during HCOOH-RMBS measurements. HCOOH beam was impinged onto the inert flag for 5 s (from 30 to 35 s) and then onto the sample surface for 5 s (from 65 to 70 s). HCOOH flux was $\sim 5 \times 10^{14}$ molecules cm^{-2} s^{-1}. Panels a−d have the same ordinate scale.

When the HCOOH molecular beam struck the inert flag, QMS signals for $m/z^+ = 46$, 44, and 28 were observed, in which the $m/z^+ = 46$ signal is the parent mass of HCOOH and the $m/z^+ = 44$ and 28 signals are mass fragments of HCOOH from QMS ionizer dissociation (similar m/z^+ ratios for masses 46, 44, and 28 were observed when shooting the HCOOH beam directly into QMS). The $m/z^+ = 18$ signal is due to a water impurity in the HCOOH[32] as we observed this mass signal when shooting the HCOOH beam directly into QMS as well. As expected, no QMS signal for H_2 ($m/z^+ = 2$) was observed when scattering the beam from the inert flag. After removing the inert flag, the HCOOH beam was directed onto the annealed 1 ML Pd/Au(111) surface, where a QMS signal for

dx.doi.org/10.1021/ja505192v | J. Am. Chem. Soc. 2014, 136, 11070−11078

H_2 production (m/z^+ = 2) was observed (Figure 3a). The emergence of the H_2 QMS signal clearly shows that the dehydrogenation reaction occurred on the 1 ML Pd/Au(111) surface. Apart from H_2 production, CO_2 (the byproduct of HCOOH dehydrogenation) and CO (the byproduct product from HCOOH dehydration) also formed as indicated by comparison of m/z^+ = 44 and 28 signals for impingement of the HCOOH beam on the inert flag and on the Pd–Au surface. These results show that the presence of Pd adatoms on the Pd–Au surface can facilitate HCOOH decomposition since no reactivity was observed on the Au(111) surface under the same testing conditions (Figure S3, Supporting Information). It is noted that formation of H_2O due to HCOOH dehydration was difficult to observe in this system, which likely results from efficient pumping of H_2O by the cryogenic probe cooled by liquid nitrogen.

Figure 3b–d shows the HCOOH-RMBS results for Pd–Au surfaces with higher initial coverages of Pd (i.e., 2–4 ML). For convenience of comparison, the integrals of QMS intensities for each species produced (i.e., H_2, CO_2, and CO) during HCOOH-RMBS (Figure 3) are summarized in Figure 4.

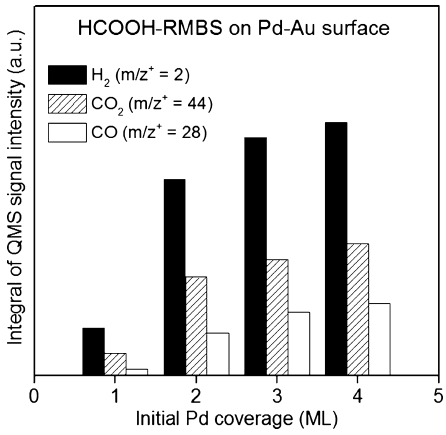

Figure 4. Integrals of QMS signal intensities for H_2, CO, and CO_2 produced on annealed Pd/Au(111) surfaces with various initial Pd coverages during HCOOH-RMBS (Figure 3).

The amount of H_2, CO_2, and CO generated on the Pd–Au surface increased as the initial Pd coverage was increased, suggestive of an activity enhancement for overall HCOOH decomposition. By comparing the m/z^+ = 46 signals obtained from the HCOOH beam impinging on the inert flag and on the sample surface, conversion of HCOOH on each surface can be estimated. As listed in Table 1, the estimated single-collision conversion of HCOOH on the Pd–Au surface increased from 0.7% to 8.8% as the initial Pd coverage was increased from 1 to 4 ML.

Figure 5a depicts the rate of HCOOH decomposition as a function of the relative number of surface Pd atoms on Pd–Au surfaces. The rate of HCOOH decomposition is the product of the conversion of HCOOH and the flux of the HCOOH molecular beam (~5 × 10^{14} molecules cm^{-2} s^{-1}) in HCOOH-RMBS experiments. As illustrated in Figure 5a, the rate of HCOOH decomposition increased as the relative number of surface Pd atoms increased. A sharp increase in the rate of HCOOH decomposition was observed when the relative number of surface Pd atoms was larger than 0.32 (i.e., the annealed 1 ML Pd/Au(111) surface). Taking the relative number of Pd–Au interface and Pd(111)-like sites into

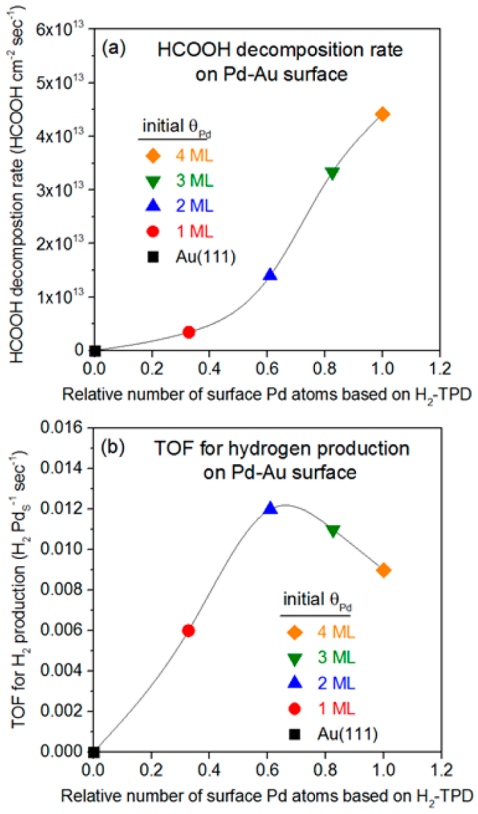

Figure 5. (a) Rate of HCOOH decomposition and (b) turnover frequency for H_2 production on Pd–Au surfaces during HCOOH-RMBS experiments shown in Figure 3.

account, this sharp increase in the HCOOH decomposition rate observed here is believed to be related to formation of Pd(111)-like sites on the Pd–Au surface. In other words, Pd(111)-like sites are more catalytically active for HCOOH decomposition than Pd–Au interface sites.

The specific activity of Pd–Au surfaces for H_2 production is expressed in terms of turnover frequency (TOF_{H2}) or the number of H_2 molecules produced per surface Pd site (Pd_S) per unit time. In this study, the TOF_{H2} on Pd–Au surfaces was computed from the integral of QMS signal intensities for H_2 production from HCOOH-RMBS experiments and H_2 desorption from TPD measurements (details associated with these calculations can be found in the Supporting Information). Figure 5b displays the calculated TOF_{H2} of each Pd–Au surface as a function of the relative number of surface Pd atoms on the Pd–Au surface. With the increase of the relative number of surface Pd atoms, the TOF_{H2} first increased to 0.012 H_2 Pd_S^{-1} s^{-1} and then slightly decreased to 0.009 H_2 Pd_S^{-1} s^{-1}. Because the rate of HCOOH decomposition increased monotonically (Figure 5a), the decrease in TOF_{H2} observed here suggests that the activity of HCOOH dehydration was enhanced, causing the selectivity for hydrogen production to be reduced as the relative number of surface Pd atoms increased.

The selectivity for H_2 production via HCOOH decomposition depends directly on the fraction of Pd atoms that exist at the Pd–Au interface or Pd(111)-like sites on the Pd–Au surface. The selectivity for hydrogen production (or dehydrogenation selectivity) can be expressed by the relative H_2/CO or CO_2/CO QMS area ratios (relative to that of the annealed 4 ML Pd/Au(111) surface) in HCOOH-RMBS experiments. Figure 6 shows the relative H_2/CO QMS area ratios and the

dx.doi.org/10.1021/ja505192v | J. Am. Chem. Soc. 2014, 136, 11070–11078

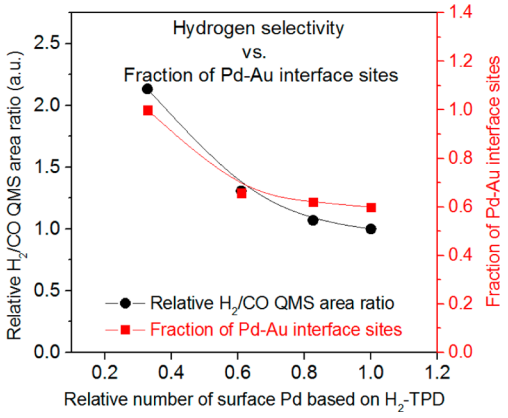

Figure 6. (a) Relative H_2/CO QMS area ratios measured from HCOOH-RMBS experiments (Figure 3), and (b) fraction of Pd–Au interface sites on Pd–Au surfaces determined by H_2-TPD measurements (Figure 1).

fraction of Pd–Au sites on Pd–Au surfaces as a function of the relative number of surface Pd atoms (the trends of relative H_2/CO and CO_2/CO QMS area ratios were almost identical, Figure S4, Supporting Information).

Figure 6 shows that the relative QMS ratio of H_2/CO, the selectivity toward hydrogen production, decreased with increasing relative number of surface Pd atoms. This decrease in hydrogen selectivity correlates with a decrease in the fraction of Pd atoms that exist as Pd–Au interface sites, suggesting that HCOOH dehydrogenation occurs at Pd–Au interface sites on the surface. The observations based on H_2-TPD and HCOOH-RMBS correlate the structure of Pd–Au surfaces with their catalytic properties on HCOOH decomposition: (1) the presence of Pd–Au interface sites on Pd–Au surfaces is crucial for selective HCOOH dehydrogenation; (2) formation of Pd(111)-like sites on Pd–Au surfaces enhances the overall HCOOH decomposition at the expense of the dehydrogenation selectivity. It is noted that high selectivity for HCOOH dehydrogenation was reported in some studies employing supported monometallic Pd catalysts.[17,19,21] Since the catalytic performance of supported monometallic metal catalysts often results from an accumulative contribution from both metal nanoparticles and the support used, the observed high selectivity[17,19,21] may be due to participation of the support in the surface reaction or metal–support interactions.

Our experimental observations are conceptually consistent with a recent theoretical study.[30] Using density function theory (DFT) methods, Yuan and Liu[30] calculated the potential energy profile for possible reaction pathways for HCOOH decomposition on four different surfaces: the Pd(111) surface, the Pd monolayer supported on the Au(111) surface (abbreviated Pd ML), and two Pd-decorated Au(111) surfaces (abbreviated Pd_6Au_3 and Pd_3Au_6). Energy barriers for HCOOH activation to form formate (HCOO) (via O–H bond cleavage) or carboxyl (COOH) intermediates (via C–H bond cleavage) are lower on the Pd(111) and Pd ML surfaces in comparison to those on the Pd_6Au_3 and Pd_3Au_6 surfaces.[30] These results support our observations that the rate of the HCOOH decomposition is enhanced by formation of Pd(111)-like sites on the Pd–Au surface. They also found that the energy barriers for further decomposition of HCOO or COOH intermediate to CO_2 and H are comparable for all surfaces investigated; however, higher energy barriers are required for dissociation of COOH into CO and OH on the Pd_6Au_3 and Pd_3Au_6 surfaces (~1 eV) than on the Pd(111) and Pd ML surfaces (~0.5–0.6 eV).[30] In other words, the dehydration pathway is inhibited relative to the dehydrogenation pathway on the Pd_6Au_3 and Pd_3Au_6 surfaces, which is consistent with the importance of Pd–Au interface sites for HCOOH dehydrogenation selectivity (Figure 6).

The catalytic properties of bimetallic catalysts are often discussed in terms of the ligand (or electronic) effect and ensemble (or geometric) effect.[28,63,64] The ligand effect describes electronic modifications caused by formation of heterometallic bonding, which leads to a charge transfer between the metals.[28] As mentioned earlier, the ligand effect has been suggested to explain the catalytic performance of Pd–Au catalysts observed for HCOOH decomposition.[19,23] Nevertheless, it is noted that the work functions for Au and Pd are similar,[11,38] and their electronegativities are identical.[38] Furthermore, XPS spectra indicate that very little (<0.2 eV) or no shifts occur in the binding energies of Pd(3d) and Au(4f) or Pd Auger electrons on Pd–Au surfaces,[36] which implies a very limited charge transfer between Pd and Au in Pd–Au alloys. The ensemble effect depicts that the atoms that exist in a particular arrangement are required for facilitating a particular catalytic process.[28] The ensemble effect for HCOOH decomposition on Pd–Au surfaces has been investigated theoretically by DFT calculations.[30] In this study, we have experimentally shown that the fraction of Pd atoms that exist in Pd–Au interface or Pd(111)-like sites has a significant influence on the reactivity and selectivity of HCOOH decomposition on the Pd–Au surface. Pd atoms in Pd(111)-like sites, which lack neighboring Au atoms, were found to exhibit a higher catalytic activity for HCOOH decomposition (Figure 5a) via the undesired dehydration pathway, resulting in a lower selectivity for hydrogen production. Pd atoms that exist at the Pd–Au interface display a lower activity for overall HCOOH decomposition but enhanced dehydrogenation selectivity (Figure 6). These observations suggest that the ensemble effect plays an important role in determining the catalytic properties of Pd–Au catalysts for selective HCOOH decomposition.

3.3. HCOOH-TPD from Pd–Au Surfaces. The interactions of HCOOH with transition metal surfaces have been extensively studied using HCOOH-TPD as reviewed by Madix,[65] Barteau,[66] and Columbia and Thiel.[67] CO_2 desorption from metal surfaces during HCOOH decomposition is typically a reaction-limited process, i.e., CO_2 desorbs immediately upon formation.[67] Thus, the catalytic activities of metal surfaces for HCOOH decomposition are frequently characterized by the desorption temperature of CO_2, where lower temperatures for CO_2 desorption are indicative of higher activities for HCOOH decomposition.[65,66] The interactions of HCOOH with low-index single-crystal surfaces of Pd have been investigated.[68–73] It was reported that the temperature for CO_2 desorption from HCOOH decomposition is ~240–260 K on the Pd(111) surface,[68,69] ~237 K on the Pd(110) surface,[70] and ~180 K on the Pd(100) surface.[71] These results suggest that the reactivity of Pd surfaces for HCOOH decomposition is sensitive to the arrangement of surface Pd atoms and the (100) facet is the most active among these structures.

Figure 7 shows the TPD spectra for various species following adsorption of 2.6 ML of HCOOH on the clean Au(111) surface and annealed 2 ML Pd/Au(111) surface.

dx.doi.org/10.1021/ja505192v | J. Am. Chem. Soc. 2014, 136, 11070–11078

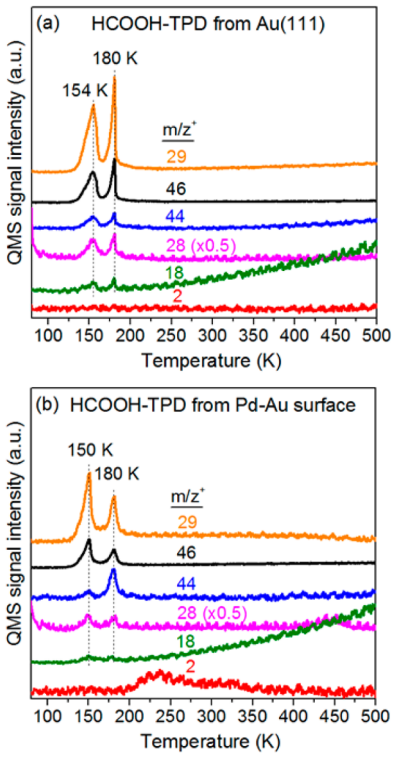

Figure 7. TPD spectra of HCOOH from the (a) Au(111) and (b) Pd–Au surfaces. The Pd–Au surface was prepared by depositing 2 ML of Pd onto the Au(111) surface at a surface temperature (T_S) of 77 K followed by annealing to 500 K in ultrahigh vacuum. Each surface was dosed with ~2.6 ML of HCOOH at T_S = 77 K. Heating rate was 1 K/s. Panels a and b have the same ordinate scale.

As shown in Figure 7a, the desorption spectrum for the parent mass of HCOOH (m/z^+ = 46) from the Au(111) surface displayed peaks at 154 and 180 K, which are due to desorption of multilayer and monolayer HCOOH, respectively (Figure S2, Supporting Information). We suggest that the observed m/z^+ = 44 and 28 signals originate from the mass fragments of HCOOH rather than from formation of CO_2 and CO because of the following: (1) the desorption temperatures of m/z^+ = 44 and 28 signals line up with those of the m/z^+ = 46 and 29 (the most intense mass fragment of HCOOH), and (2) the ratios of integral intensities of these QMS signals are similar to those obtained from the HCOOH beam impingement onto the inert flag. No measurable H_2 (m/z^+ = 2) desorption was observed during TPD from the HCOOH-precovered Au(111) surface. As mentioned earlier, the observed signal for m/z^+ = 18 was due to the water impurity in HCOOH. Results in Figure 7a confirm that the Au(111) surface is inactive for HCOOH decomposition during TPD measurements, which is also consistent with observations from the HCOOH-RMBS experiment on the clean Au(111) surface (Figure S3, Supporting Information) and with reports that HCOOH interacts weakly with the clean Au(111) surface using XPS and RAIRS.[74]

TPD spectra of HCOOH from the Pd–Au surface were measured under the same set of conditions (Figure 7b). Significant attenuation of the desorption feature for the HCOOH monolayer at ~180 K indicates that HCOOH decomposed on this surface. The small peak in the m/z^+ = 28 signal at ~450 K is due to desorption of CO adsorbed on the surface from the background gas[35] or from decomposition of HCOOH. It is noted that the m/z^+ = 44 spectrum is dissimilar from the m/z^+ = 46, 29, and 28 spectra. The pronounced signal for m/z^+ = 44 at ~180 K shows that CO_2 molecules evolved from the Pd–Au surface during heating. CO_2 evolution observed here is a reaction-limited process rather than a desorption-limited process as CO_2 molecules desorb at much lower temperatures from Au(111)[75] and Pd(111) surfaces.[76] Thus, CO_2 desorption occurred immediately upon its formation, which was due to decomposition of the reaction intermediate(s) such as formate (HCOO) and carboxyl (COOH).[30] Unfortunately, we were unable to identify the reactive intermediate(s) on the Pd–Au surface via RAIRS (Figure S5, Supporting Information) due to the small surface concentration of these intermediates which gave a low signal-to-noise ratio. The temperature of CO_2 evolution via HCOOH decomposition from the Pd–Au surface (~180 K) is coincident with that from the Pd(100) surface,[71] which suggests that the Pd–Au surface is comparably active to the Pd(100) surface for HCOOH decomposition during heating.

4. CONCLUSIONS

We conducted a model catalyst study to investigate the reactivity of HCOOH on a variety of Pd–Au bimetallic surfaces using temperature-programmed desorption and reactive molecular beam scattering. Our results reveal that Pd atoms are the active component for HCOOH decomposition on the Pd–Au alloy surface. The selectivity of the reaction is governed by the type of the nearest neighbor atoms adjacent to the Pd atoms. Pd atoms which lack adjacent Au atoms favor dehydration of HCOOH, whereas Pd atoms that possess Au atoms as nearest neighbors favor dehydrogenation of HCOOH, which is desirable for efficient production of hydrogen. These observations suggest that the reactivity and selectivity of HCOOH decomposition on Pd–Au bimetallic catalysts could be optimized by controlling the arrangement of Pd and Au atoms on the surface through the ensemble effect. We believe these findings will be beneficial for the future design of Pd–Au bimetallic catalysts for associated reactions including selective HCOOH decomposition for hydrogen production and electro-oxidation of HCOOH in the direct formic acid fuel cell.[77] We hope our observations will inspire more advanced surface characterization to further investigate the relationship between the catalytic activities and the surface nature of Pd–Au surfaces.

■ ASSOCIATED CONTENT

Supporting Information

Additional information regarding AES characterization for the as-deposited and annealed Pd/Au(111) surfaces, TPD of HCOOH from the Au(111) surface, RMBS of HCOOH on the Au(111) surface, derivation of equations for calculating TOF_{H2}, relative H_2/CO and CO_2/CO QMS area ratios for RMBS of HCOOH on Pd–Au surfaces, RAIRS of HCOOH on the Au(111) and annealed Pd/Au(111) surfaces; AES spectra for the as-deposited and annealed Pd/Au(111) surface with various initial Pd coverages; HCOOH-TPD spectra from the Au(111) surface; HCOOH-RMBS results for the Au(111) surface; relative H_2/CO and CO_2/CO QMS area ratios measured from Pd–Au surfaces in HCOOH-RMBS experiments; RAIRS spectra of HCOOH on the Au(111) and annealed 2 ML Pd/Au(111) surfaces. This material is available free of charge via the Internet at http://pubs.acs.org.

AUTHOR INFORMATION

Corresponding Author

E-mail: mullins@che.utexas.edu

Notes

The authors declare no competing financial interest.

ACKNOWLEDGMENTS

We are thankful for the generous support of the Department of Energy (DE-FG02-04ER15587) and the Welch Foundation (Grant F-1436). G.M.M. thanks the National Science Foundation for a Graduate Research Fellowship.

REFERENCES

(1) Enthaler, S. *ChemSusChem* **2008**, *1*, 801−804.
(2) Joo, F. *ChemSusChem* **2008**, *1*, 805−808.
(3) Enthaler, S.; von Langermann, J.; Schmidt, T. *Energy Environ. Sci.* **2010**, *3*, 1207−1217.
(4) Loges, B.; Boddien, A.; Gartner, F.; Junge, H.; Beller, M. *Top. Catal.* **2010**, *53*, 902−914.
(5) Johnson, T. C.; Morris, D. J.; Wills, M. *Chem. Soc. Rev.* **2010**, *39*, 81−88.
(6) Boddien, A.; Loges, B.; Gartner, F.; Torborg, C.; Fumino, K.; Junge, H.; Ludwig, R.; Beller, M. *J. Am. Chem. Soc.* **2010**, *132*, 8924−8934.
(7) Boddien, A.; Gartner, F.; Jackstell, R.; Junge, H.; Spannenberg, A.; Baumann, W.; Ludwig, R.; Beller, M. *Angew. Chem., Int. Ed.* **2010**, *49*, 8993−8996.
(8) Boddien, A.; Mellmann, D.; Gartner, F.; Jackstell, R.; Junge, H.; Dyson, P. J.; Laurenczy, G.; Ludwig, R.; Beller, M. *Science* **2011**, *333*, 1733−1736.
(9) Hull, J. F.; Himeda, Y.; Wang, W. H.; Hashiguchi, B.; Periana, R.; Szalda, D. J.; Muckerman, J. T.; Fujita, E. *Nat. Chem.* **2012**, *4*, 383−388.
(10) Boddien, A.; Junge, H. *Nat. Nanotechnol.* **2011**, *6*, 265−266.
(11) Tedsree, K.; Li, T.; Jones, S.; Chan, C. W. A.; Yu, K. M. K.; Bagot, P. A. J.; Marquis, E. A.; Smith, G. D. W.; Tsang, S. C. E. *Nat. Nanotechnol.* **2011**, *6*, 302−307.
(12) Zhou, X. C.; Huang, Y. J.; Xing, W.; Liu, C. P.; Liao, J. H.; Lu, T. H. *Chem. Commun.* **2008**, 3540−3542.
(13) Huang, Y. J.; Zhou, X. C.; Yin, M.; Liu, C. P.; Xing, W. *Chem. Mater.* **2010**, *22*, 5122−5128.
(14) Zhou, X. C.; Huang, Y. J.; Liu, C. P.; Liao, J. H.; Lu, T. H.; Xing, W. *ChemSusChem* **2010**, *3*, 1379−1382.
(15) Gu, X. J.; Lu, Z. H.; Jiang, H. L.; Akita, T.; Xu, Q. *J. Am. Chem. Soc.* **2011**, *133*, 11822−11825.
(16) Yadav, M.; Singh, A. K.; Tsumori, N.; Xu, Q. *J. Mater. Chem.* **2012**, *22*, 19146−19150.
(17) Bulushev, D. A.; Beloshapkin, S.; Ross, J. R. H. *Catal. Today* **2010**, *154*, 7−12.
(18) Bulushev, D. A.; Jia, L. J.; Beloshapkin, S.; Ross, J. R. H. *Chem. Commun.* **2012**, *48*, 4184−4186.
(19) Bulushev, D. A.; Beloshapkin, S.; Plyusnin, P. E.; Shubin, Y. V.; Bukhtiyarov, V. I.; Korenev, S. V.; Ross, J. R. H. *J. Catal.* **2013**, *299*, 171−180.
(20) Zhao, Y.; Deng, L.; Tang, S. Y.; Lai, D. M.; Liao, B.; Fu, Y.; Guo, Q. X. *Energy Fuels* **2011**, *25*, 3693−3697.
(21) O'Neill, B. J.; Gürbüz, E. I.; Dumesic, J. A. *J. Catal.* **2012**, *290*, 193−201.
(22) Metin, O.; Sun, X. L.; Sun, S. H. *Nanoscale* **2013**, *5*, 910−912.
(23) Wang, Z. L.; Yan, J. M.; Wang, H. L.; Ping, Y.; Jiang, Q. *J. Mater. Chem. A* **2013**, *1*, 12721−12725.
(24) Campbell, C. T. *Annu. Rev. Phys. Chem.* **1990**, *41*, 775−837.
(25) Somorjai, G. A. *Chem. Rev.* **1996**, *96*, 1223−1235.
(26) Weaver, J. F.; Carlsson, A. F.; Madix, R. J. *Surf. Sci. Rep.* **2003**, *50*, 107−199.
(27) Gong, J. L. *Chem. Rev.* **2012**, *112*, 2987−3054.
(28) Gao, F.; Goodman, D. W. *Chem. Soc. Rev.* **2012**, *41*, 8009−8020.
(29) Pan, M.; Brush, A. J.; Pozun, Z. D.; Ham, H. C.; Yu, W.-Y.; Henkelman, G.; Hwang, G. S.; Mullins, C. B. *Chem. Soc. Rev.* **2013**, *42*, 5002−5013.
(30) Yuan, D. W.; Liu, Z. R. *J. Power Sources* **2013**, *224*, 241−249.
(31) Flaherty, D. W.; Hahn, N. T.; Ferrer, D.; Engstrom, T. R.; Tanaka, P. L.; Mullins, C. B. *J. Phys. Chem. C* **2009**, *113*, 12742−12752.
(32) Flaherty, D. W.; Berglund, S. P.; Mullins, C. B. *J. Catal.* **2010**, *269*, 33−43.
(33) Flaherty, D. W.; Yu, W.-Y.; Pozun, Z. D.; Henkelman, G.; Mullins, C. B. *J. Catal.* **2011**, *282*, 278−288.
(34) Yu, W.-Y.; Mullen, G. M.; Mullins, C. B. *J. Phys. Chem. C* **2013**, *117*, 19535−19543.
(35) Yu, W.-Y.; Mullen, G. M.; Mullins, C. B. *J. Phys. Chem. C* **2014**, *118*, 2129−2137.
(36) Koel, B. E.; Sellidj, A.; Paffett, M. T. *Phys. Rev. B* **1992**, *46*, 7846−7856.
(37) Baddeley, C. J.; Ormerod, R. M.; Stephenson, A. W.; Lambert, R. M. *J. Phys. Chem.* **1995**, *99*, 5146−5151.
(38) Chen, M. S.; Kumar, D.; Yi, C. W.; Goodman, D. W. *Science* **2005**, *310*, 291−293.
(39) Christmann, K. Introduction to Surface Physical Chemistry, In *Topics in Physical Chemistry*; Springer: New York, 1991; pp 152−166.
(40) Masel, R. I. Principles of Adsorption and Reaction on Solid Surfaces. In *Wiley Series in Chemical Engineering*; John Wiley & Sons, Inc.: New York, 1996; pp 507−515.
(41) Attard, G.; Barnes, C., Surfaces. *Oxford Chemistry Primers 59*; Oxford University Press: Oxford, 1998; pp 71−75.
(42) Kleyn, A. W. *Chem. Soc. Rev.* **2003**, *32*, 87−95.
(43) Libuda, J.; Freund, H. J. *Surf. Sci. Rep.* **2005**, *57*, 157−298.
(44) Yi, C. W.; Luo, K.; Wei, T.; Goodman, D. W. *J. Phys. Chem. B* **2005**, *109*, 18535−18540.
(45) Wei, T.; Wang, J.; Goodman, D. W. *J. Phys. Chem. C* **2007**, *111*, 8781−8788.
(46) Gao, F.; Wang, Y. L.; Goodman, D. W. *J. Am. Chem. Soc.* **2009**, *131*, 5734−5735.
(47) Li, Z.; Gao, F.; Furlong, O.; Tysoe, W. T. *Surf. Sci.* **2010**, *604*, 136−143.
(48) Sellidj, A.; Koel, B. E. *Phys. Rev. B* **1994**, *49*, 8367−8376.
(49) Baddeley, C. J.; Tikhov, M.; Hardacre, C.; Lomas, J. R.; Lambert, R. M. *J. Phys. Chem.* **1996**, *100*, 2189−2194.
(50) Behm, R. J. *Z. Phys. Chem.* **2009**, *223*, 9−36.
(51) Boscoboinik, J. A.; Calaza, F. C.; Garvey, M. T.; Tysoe, W. T. *J. Phys. Chem. C* **2010**, *114*, 1875−1880.
(52) Ogura, S.; Okada, M.; Fukutani, K. *J. Phys. Chem. C* **2013**, *117*, 9366−9371.
(53) Pan, M.; Flaherty, D. W.; Mullins, C. B. *J. Phys. Chem. Lett.* **2011**, *2*, 1363−1367.
(54) Gdowski, G. E.; Felter, T. E.; Stulen, R. H. *Surf. Sci.* **1987**, *181*, L147−L155.
(55) Tierney, H. L.; Baber, A. E.; Kitchin, J. R.; Sykes, E. C. H. *Phys. Rev. Lett.* **2009**, *103*, 246102.
(56) Baber, A. E.; Tierney, H. L.; Lawton, T. J.; Sykes, E. C. H. *ChemCatChem.* **2011**, *3*, 607−614.
(57) Mullins, C. B.; Weinberg, W. H. *J. Chem. Phys.* **1990**, *92*, 3986−3988.
(58) Rettner, C. T.; Mullins, C. B.; Bethune, D. S.; Auerbach, D. J.; Schweizer, E. K.; Weinberg, W. H. *J. Vac. Sci. Technol. A* **1990**, *8*, 2699−2704.
(59) Mullins, C. B.; Rettner, C. T.; Auerbach, D. J.; Weinberg, W. H. *Chem. Phys. Lett.* **1989**, *163*, 111−115.
(60) Sitz, G. O.; Mullins, C. B. *J. Phys. Chem. B* **2002**, *106*, 8349−8353.
(61) Davis, J. E.; Karseboom, S. G.; Nolan, P. D.; Mullins, C. B. *J. Chem. Phys.* **1996**, *105*, 8362−8375.
(62) Wheeler, M. C.; Seets, D. C.; Mullins, C. B. *J. Chem. Phys.* **1996**, *105*, 1572−1583.
(63) Liu, P.; Norskov, J. K. *Phys. Chem. Chem. Phys.* **2001**, *3*, 3814−3818.

(64) Ham, H. C.; Hwang, G. S.; Han, J.; Nam, S. W.; Lim, T. H. *J. Phys. Chem. C* **2010**, *114*, 14922−14928.
(65) Madix, R. J. *Adv. Catal.* **1980**, *29*, 1−53.
(66) Barteau, M. A. *Catal. Lett.* **1991**, *8*, 175−184.
(67) Columbia, M. R.; Thiel, P. A. *J. Electroanal. Chem.* **1994**, *369*, 1−14.
(68) Davis, J. L.; Barteau, M. A. *Surf. Sci.* **1991**, *256*, 50−66.
(69) Jeroro, E.; Vohs, J. M. *Catal. Lett.* **2009**, *130*, 271−277.
(70) Aas, N.; Li, Y. X.; Bowker, M. *J. Phys. Condens. Matter* **1991**, *3*, S281−S286.
(71) Sander, D.; Erley, W. *J. Vac. Sci. Technol. A* **1990**, *8*, 3357−3360.
(72) Jorgensen, S. W.; Madix, R. J. *J. Am. Chem. Soc.* **1988**, *110*, 397−400.
(73) Solymosi, F.; Kovacs, I. *Surf. Sci.* **1991**, *259*, 95−108.
(74) Senanayake, S. D.; Stacchiola, D.; Liu, P.; Mullins, C. B.; Hrbek, J.; Rodriguez, J. A. *J. Phys. Chem. C* **2009**, *113*, 19536−19544.
(75) Farkas, A. P.; Solymosi, F. *J. Phys. Chem. C* **2009**, *113*, 19930−19936.
(76) Wambach, J.; Odorfer, G.; Freund, H. J.; Kuhlenbeck, H.; Neumann, M. *Surf. Sci.* **1989**, *209*, 159−172.
(77) Larsen, R.; Ha, S.; Zakzeski, J.; Masel, R. I. *J. Power Sources* **2006**, *157*, 78−84.